The scale-up of Cr^{3+} biosorption onto olive stone in a fixed bed column

Mónica Calero, Alicia Ronda*, Antonio Pérez, Andrés Yáñez, M. Carmen Trujillo, María Ángeles Martín-Lara

Department of Chemical Engineering, University of Granada, Granada 18071, Spain, Tel. +34 958 243315; Fax: +34 958 248992; emails: mcaleroh@ugr.es (M. Calero), alirg@ugr.es (A. Ronda), Tel. +34 958 244075; Fax: +34 958 248992; email: aperezm@ugr.es (A. Pérez), Tel. +34 958 243315; Fax: +34 958 248992; emails: aamador@correo.ugr.es (A. Yáñez), mariac.trujillo@hotmail.com (M.C. Trujillo), Tel. +34 958 240445; Fax: +34 958 248992; email: marianml@ugr.es (M.Á. Martín-Lara)

ABSTRACT

In this work, the scale up of olive stone columns for water purification, based on results from the biosorption of Cr(III) onto olive stone in a fixed bed column at pilot scale, was developed. Pilot-scale experiments were carried out in a fixed bed column to test the influence of various parameters (flow rate, bed depth, and initial chromium concentration) on breakthrough curves. Mathematical relationships were developed to describe Cr(III) biosorption in fixed bed column of olive stone at pilot scale. The results were found to be consistent with the previous published results obtained from laboratory scale. The bed depth service time (BDST), the Adams–Bohart, the Thomas, the Yoon and Nelson, and the Dose–Response models were used to analyze the experimental data and the model parameters were evaluated. The BDST allowed comparison between performances of pilot- and laboratory-scale columns, and Dose–Response model showed good agreement of the experimental breakthrough curves with model predictions. The results showed that when the initial Cr(III) concentration was increased from 10 to 80 mg/L, the corresponding biosorption bed capacity increased from 0.126 to 0.262 mg/g at constant flow rate and bed depth. Also, breakthrough time varies from 30 to 220 min when the bed height increases from 21.5 to 62.0 cm at constant flow rate and initial Cr(III) concentration. Results showed that scale up multiplied by nearly 1.7 the important parameters as critical bed depth and length of unused bed (the same relation that the ratio between length/diameter of pilot-scale column and laboratory-scale column).

Keywords: Biosorption; Breakthrough curve; Chromium (III); Fixed bed column; Olive stone; Scale up

1. Introduction

Due to the increasing level of toxic metals found in residual streams originated from industrial discharges, new methods and techniques are developed for environmental control [1]. Metal biosorption by agricultural or forestry solids is one of the most useful options for this type of problems.

In this work, the olive stone is used as solid biosorbent, which is obtained as a byproduct of the production of olive oil. This biosorbent has a particular interest both economically and environmentally,

*Corresponding author.

especially if it is considered the high amount produced in Andalusia (Spain) and the little or no value that it has currently.

In addition, even though several publications have reported biosorption for water treatment in batch systems [2–6], nowadays biosorption in fixed bed columns is preferable for industrial water treatment [7]. Moreover, to optimize the process, it is necessary to perform scale-up studies that can be used for industrial equipment.

Scale up stands a much better chance for success, if the laboratory and large-scale units are carried out in the same type of system, for example, fixed-bed, fluidized-bed, and batch reactors [8]. From this point of view, keeping the same column type at different scales, the critical parameter is the column size, which incorporates its geometrical analogies and dimensions. Neither furthermore, in this case of biosorption in fixed beds, the fact that no heat transfer occurs is crucial as this operation is essentially isothermal. Thus, scale up mainly takes into account mass-transfer phenomena, and of course the hydraulic performance of the column (mainly liquid distribution).

Various methods can be employed in modeling chemical or physical processes. There are three basic approaches in the scale-up procedure [9]: (a) "mathematical modeling", (b) "physical modeling", and (c) "experimental scale up". The first stage in the mathematical modeling of a process is to express mathematically the relationship between the basic process variables and the boundary conditions and set up an algorithm. The second step consists of changing the various parameters, using the algorithm, to check whether the model corresponds to the process investigated and to select the optimal conditions. Physical modeling is an alternative to the mathematical one, when the latter is not applicable. Two different methods can be followed in the context of physical modeling: (a) the similarity method, and (b) the dimensional analysis. Finally, experimental scale up can be seen as part of physical and scale-up modeling. In the following, its methodology is briefly presented: (a) a carefully planned test campaign is needed to collect data that adequately cover a wide range of the most important operating variables, conducting the minimum possible experiments, (b) the next step is the selection of the appropriate mathematical expression form and, subsequently, the process parameters should be estimated by minimizing the differences between the values predicted from the selected mathematical expression and the data experimentally found. Then, an extensive pilot-plant study is usually undertaken. It is during pilot-plant experiments when scale-up problems must be dealt with adequately. Under specified conditions, the data of the pilot-scale unit can be used for the evaluation of the large-scale unit performance.

In this work, specific research objectives were to: (1) evaluate the effects of feed flow rate, bed depth, and inlet metal concentrations on Cr(III) removal in a pilot-scale fixed-bed column packed with olive stone, (2) develop an "experimental scale up" of Cr(III) breakthrough data (the dynamical behavior can be described in terms of time–concentration profiles commonly called breakthrough curves) obtained with pilot-scale column tests, (3) compare results obtained on pilot-scale column tests with those obtained on laboratory scale in previous published works, and (4) assess about the use of mathematical correlations obtained in the process of "experimental scale up" to predict the behavior of an industrial-scale unit.

2. Experimental

2.1. Biosorbent: olive stone

Olive stones were supplied by the olive cake oil extraction plant "Cooperativa Nuestra Señora del Castillo" located in Vilches, province of Jaén, Spain.

The stones were obtained from the separation process of the olive cake with an industrial pitting machine, with a 4-mm sieve separator, which is the standard size used in this industrial process. Then, the olive stones were milled with an analytical mill (IKA MF-10) and the fraction lower than 1 mm was chosen for all the tests. An average particle size of 0.757 mm was calculated according the particle distribution of the solid.

A deep characterization of the OS has been performed in previous works [10,11]. In this work, a summary table is included with main data from chemical–physical characterization of OS (Table 1).

2.2. Solutions preparations

Cr(III) solutions were prepared by dissolving 9-hidrate chromium nitrate [Cr(NO$_3$)$_3$·9H$_2$O] in distilled water. According to a previous work [3], the pH of the solutions was adjusted to 4 with 0.1 N solutions of NaOH and HCl. All chemicals used in this work were of analytical grade (supplied by Panreac).

2.3. Column experiments

In a previous paper, [12] experiments have been conducted to analyze the biosorption of Cr(III) using a laboratory-scale fixed bed. In this work, the fixed-bed

Table 1
Physical and chemical properties of olive stone [10,11]

Property		OS
BET surface area	Total surface area, m^2/g	0.163
	Internal surface, m^2/g	0.140
	External surface, m^2/g	0.022
Total porous volume, cm^3/g		1.84×10^{-3}
Pore diameter, Å		453.02
Structural components	Lignin, g/kg free extracts	403.80
	Cellulose, g/kg free extracts	271.40
	Hemicellulose, g/kg free extracts	321.80
Particle size distribution, %	>1.000 mm	17.52
	1.000–0.710 mm	42.13
	0.710–0.500 mm	18.04
	0.500–0.355 mm	5.09
	0.355–0.250 mm	5.40
	<0.250 mm	12.01
Elemental analysis, %	Carbon	52.34
	Hydrogen	7.11
	Nitrogen	0.03
	Sulfur	<0.10
	Oxygen	40.47
Proximate analysis, %	Moisture	5.43
	Volatile matter	74.66
	Fixed carbon	19.54
	Ash	0.37
Potentiometric titrations	Total titrables sites, mol/g	6.94×10^{-5}
	Acid titrables sites, mol/g	3.70×10^{-5}
	Basic titrables sites, mol/g	3.24×10^{-5}
	Point of zero charge (pH$_{PZC}$)	5.17
Carbon release to solution, mg C/L	Total carbon	36.84
	Total inorganic carbon	0.02
	Total organic carbon	36.82

column experiments were conducted in a pilot-scale jacket glass column packed with olive stone particles. The unit had an automatic pH controller and a system for taking samples automatically. Temperature was maintained at 25℃ by a thermostatic bath. The chromium solution at a known concentration was pumped through the column of sorbent using a peristaltic pump (Dinko, model D21V) with variable speed adjustment. Samples from the column effluent were collected at regular intervals and analyzed by atomic absorption spectrometry (Perkin Elmer Model AAnalist 200). The column studies were performed at pH 4 and the effluent pH was permanently recorded.

To perform scaling, the criteria of similarity have been followed [13]. In this focus, the work takes into account the following points:

(1) Geometric similarity: The relation between length of column (H for pilot scale columns and h for laboratory columns) and the diameter (D for pilot scale columns and d for laboratory columns) has been kept constant in both columns ($H/D = h/d$).

(2) Kinematic similarity: The physical properties of the fluid are kept constant in both columns to ensure the transfer matter regime.

(3) Dynamic similarity: As the physical properties of the fluid are the same in both columns and the used solid particles are the same type, (the same size and porosity), it holds that linear velocities, v, in both columns will be practically constants.

In Table 2, the basic design and operation parameters of the columns, laboratory and pilot scale, are collected. In order to utilize almost all the available bed length in the pilot scale column, the used amount of olive stone in this column was around 60 times higher than used in laboratory scale column. So, an amount of 300 g is equivalent to a bed depth of 21.5 cm, 600 g

Table 2
Basic design and operating parameters of the laboratory-scale and pilot-scale columns

Laboratory-scale column

$H = 23$ cm $H/D = 13.53$
$D = 1.7$ cm Section $(S) = 2.27$ cm^2
Temperature $= 25°C$

Biosorbent mass, g	Bed depth, cm	Bed volume, cm^3
$m = 5$	$Z = 4.4$	$V_b = 10.0$
$m = 10$	$Z = 8.9$	$V_b = 20.2$
$m = 15$	$Z = 13.4$	$V_b = 30.4$

Bulk density, $\rho_b = 0.510$ g/cm^3
Solid density, $\rho_s = 1.426$ g/cm^3
Bed porosity, $\varepsilon = 0.648$

Feed flow rates, mL/min	Lineal speed, cm/s
$Q = 2$ mL/min	$v = 0.881$ cm/s
$Q = 4$ mL/min	$v = 1.762$ cm/s
$Q = 6$ mL/min	$v = 2.643$ cm/s

Pilot-scale column

$H = 65$ cm $H/D = 13.83$
$D = 4.7$ cm Section $(S) = 17.35$ cm^2
Temperature $= 25°C$

Biosorbent mass, g	Bed depth, cm	Bed volume, cm^3
$m = 300$	$Z = 21.5$	$V_b = 373.0$
$m = 600$	$Z = 42.5$	$V_b = 737.3$
$m = 900$	$Z = 62.0$	$V_b = 1075.7$

Bulk density, $\rho_b = 0.804$ g/cm^3
Solid density, $\rho_s = 1.426$ g/cm^3
Bed porosity, $\varepsilon = 0.436$

Feed flow rates, mL/min	Lineal speed, cm/s
$Q = 14$ mL/min	$v = 0.807$ cm/s
$Q = 28$ mL/min	$v = 1.614$ cm/s
$Q = 46$ mL/min	$v = 2.651$ cm/s

is equivalent to a bed depth of 42.5 cm, and 900 g is equivalent to a bed depth of 62.0 cm. Therefore, the relation between obtained value of bed depth/column diameter for pilot scale column (Z/D) and laboratory column (z/d) is 1.7. This value has been taken into account in the obtained results.

With the aim to study the effect of different operational parameters of the column, the criteria of constant operational time has been followed. For it, the exhaustion of the column is not reached in some experiments; however, in this way, the trend of the breakthrough curve for a single parameter is better observed.

2.3.1. Effect of flow rate

The experimental conditions chosen to study the effect of the feed flow rate on the biosorption process in a packed column were in accordance with studies made in laboratory size columns [12]. The conditions were: inlet concentration of Cr(III), 10 mg/L; pH 4; time = 600 min; olive stone mass, 600 g (equivalent to 42.5 cm of bed depth); and feed flow rates 14, 28, and 46 mL/min.

2.3.2. Effect of bed depth

The sorption performance of olive stone was tested at various bed depths, 300 g (21.5 cm), 600 g (42.5 cm), and 900 g (62.0 cm) at a flow rate of 28 mL/min; pH 4; time = 600 min; and inlet chromium concentrations of 10 mg/L.

2.3.3. Effect of inlet Cr(III) concentration. Breakthrough curves: Modelling and determination of kinetic parameters

In modeling and determining of kinetic parameters, the following values of the operational parameters were chosen: flow rate = 14 mL/min; pH 4; time = 600 min; olive stone mass = 600 g (equivalent to a bed depth of 42.5 cm); and inlet concentrations of Cr (III) = 10, 20, 40, and 80 mg/L (the industrial water discharges may contain metal ion concentrations very different in function of the industry). For Cr(III), this range is usual in the industrial wastewater discharges.

3. Mathematical modeling

The first stage in the mathematical modeling of a process is to express mathematically the relationship between the basic process variables and the boundary conditions and set up an algorithm.

The dynamic behavior of columns is described in terms of "effluent concentration-time" profile, which it is called breakthrough curve. This breakthrough curve is usually expressed by mean a normalized concentration defined as the ratio between the metal concentrations in the liquid at the outlet and inlet of the column (C/C_i), in function of time or volume of the effluent, for a bed depth fixed.

(1) The volume of the effluent, V_{ef} (mL), can be calculated through the following equation:

$$V_{ef} = Q\, t_{total} \tag{1}$$

where t_{total} is the total flow time in min and Q is the volumetric flow rate which circulates through the column in mL/min.

(2) The area under the breakthrough curve represents the total mass of metal biosorbed, q_{total}, in mg, for a given feed concentration and flow rate and it can be determined by integration:

$$q_{total} = \frac{Q}{1000} \int_{t=0}^{t=t_{total}} C_R\, dt \tag{2}$$

where C_R is the concentration of metal removal in mg/L.

(3) The total amount of metal ions sent to the column, in mg, can be calculated from the following expression:

$$m_{total} = \frac{C_i\, Q\, t_{total}}{1000} \tag{3}$$

(4) The total metal removal (%) can be calculated from the ratio of metal mass biosorbed (q_{total}) to the total amount of metal ions sent to the column (m_{total}) as:

$$\%\,R = \frac{q_{total}}{m_{total}} \times 100 \tag{4}$$

(5) The amount of metal biosorbed at equilibrium or biosorption capacity, q_e (mg of sorbated metal/g of sorbent), and the equilibrium metal concentration, C_e (mg/L), can be determined using the following equations:

$$q_e = \frac{q_{total}}{m} \tag{5}$$

Table 3
Mathematical models to predict the dynamic behavior of the column

Model	Considerations	Equation and parameters	Refs.
Bed-depth-service-time	Model simple used to speed up the design of continuous adsorption process by reducing the amount of preliminary experiments	$t = \frac{N_0}{C_i V} Z - \frac{1}{K_a C_i} \ln\left(\frac{C_i}{C} - 1\right)$ N_0, sorption capacity of bed, mg/L K_a, rate constant, L/mg min	[14]
Adams–Bohart	This model assumes that the sorption rate is proportional to the residual capacity of the solid and the concentration of the sorbed substance and is used to describe the initial part of the breakthrough curve	$\frac{C}{C_i} = e^{k_{AB} C_i t - \frac{k_{AB} N_0 Z}{V}}$ k_{AB}, kinetics constant, L/mg min N_0, maximum volumetric sorption capacity, mg/L	[15]
Thomas	This model considers that sorption is not limited by the chemical reaction but controlled by the mass-transfer at the interface	$\frac{C}{C_i} = \frac{1}{1 + \exp\left(\frac{k_{Th}}{Q}(q_0 m - C_i V_{ef})\right)}$ k_{Th}, Thomas rate constant, mL/min mg q_0, maximum concentration of the solute in the solid phase, mg/g	[16,17]
Yoon–Nelson	This model assumes that the rate of decrease in the probability of adsorption for each adsorbate is proportional to the probability of adsorbate adsorption and the probability of adsorbate breakthrough on sorbent	$\frac{C_i}{C} = \frac{1}{1 + e^{k_{YN}(T-t)}}$ k_{YN}, Yoon–Nelson's proportionality constant, min^{-1} τ, time required for retaining 50% of the initial adsorbate, min	[18]
Dose–Response	This model, which has been commonly used in pharmacology to describe different types of processes, is currently being applied to describe the biosorption in columns	$\frac{C}{C_i} = 1 - \frac{1}{1 + \left(\frac{C_i V_{ef}}{q_0 m}\right)^a}$ a, constant of model q_0, maximum concentration of the solute in the solid phase, mg/g	[19,20]

$$C_e = \frac{m_{total} - q_{total}}{V_{ef}} \times 1000 \qquad (6)$$

where m is the mass of sorbent in g. In experiments where the equilibrium is not reached, the value q_e is related to the biosorption capacity at final contact time of the column.

(6) Exhausted time: When the volume of the fluid begins to flow through the column, the mass-transfer zone varies from 0% of the inlet concentration (corresponding to the solute-free sorbent) to 100% of the inlet concentration (corresponding to the total saturation). From a practical point of view, the exhausted time, t_{ex}, is established when the concentration of the effluent is higher than 90–95% of the inlet concentration.

(7) Service or breakthrough time: The breakthrough time, t_b, is established when the metal concentration in the effluent reaches a determined value, generally related to the permitted disposal limit for each metal. In this work, the breakthrough time has been established when the concentration of the effluent is around 2 mg/L.

Various simple mathematical models such as Adams–Bohart, Thomas, Yoon–Nelson, and Dose–Response models have been developed to predict the dynamic behavior of the column and allow some kinetic coefficients to be estimated by nonlinear regression. These models are summarized in Table 3. To choose them, it has been considered the conditions of application of each one of them and their use for the study of biosorption in a column by the majority of researchers.

4. Results and discussion

4.1. Effect of flow rate

The effect of flow rate on Cr(III) biosorption by olive stone was investigated by varying the flow rate from 14 to 46 mL/min and keeping an inlet Cr(III) concentration of 10 mg/L and a bed height of 42.5 cm (600 g of olive stone). The plots of normalized
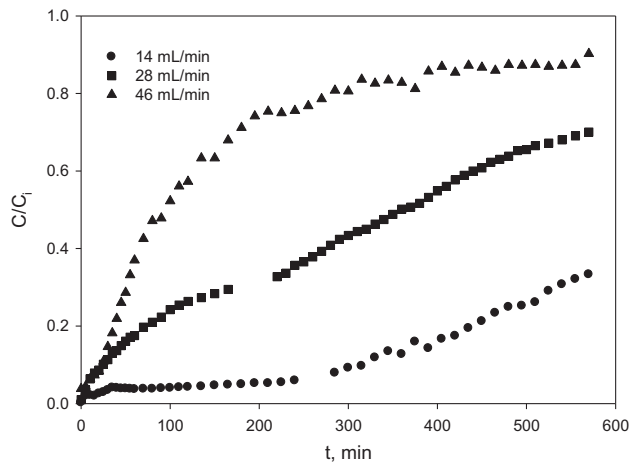
Fig. 1a. Cr(III) biosorption breakthrough curves by olive stone at three different feed flow rates (14, 28, and 46 mL/min).
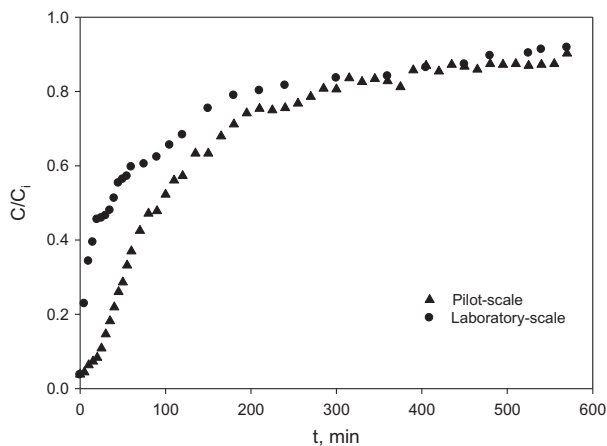

Fig. 1b. Breakthrough curves obtained in laboratory-scale column and pilot-scale column using equivalent operations conditions (Laboratory-scale: C_i = 10 mg/L; Q = 6 mL/min; Z = 8.9 cm. Pilot-scale: C_i = 10 mg/L; Q = 46 mL/min; Z = 42.5 cm).

concentration of chromium on the effluent vs. time at different flow rates are shown in Fig. 1a.

As the flow rate decreases, the retention of Cr(III) by olive stone increases (total sorbed chromium quantity and chromium removal percentage values decreased with increasing flow rate), reaching exhaustion in the column only when the flow rate is 46 mL/min, while at the other two flow rates, especially at 14 mL/min, the contact time must be prolonged to achieve exhaustion. The breakthrough time increases as the flow rate decreases, obtaining values of 450, 100, and 40 min for 14, 28, and 46 mL/min, respectively.

With increasing the flow rate the turbulence of flow begins to increase and this leads to decreasing of external film diffusion mass-transfer resistance, therefore the rate of metal ion transferred to biosorbent surface increases leading to fast saturation and earlier breakthrough time. On the other hand, when the flow rate decreases, the residence time in the column is longer as intra-particle diffusion then becomes effective. Thus, metal ion has enough time to penetrate and diffuse deeply into the pores and accordingly, better removal efficiency is obtained [21–23].

In this sense, the performance of the column was found to be consistent with the previous published results obtained from laboratory scale [12].

In Fig. 1b has been represented, by way of example, the obtained breakthrough curves in laboratory- and pilot scale columns, using similar operational conditions (using the operational conditions indicated before). It is observed that during first 200 min of operation, the retention of metal by the olive stone is faster in laboratory columns, decreasing this difference when the time increases, until obtaining similar values at final of the operational time.

4.2. Effect of bed height (or bed depth)

Accumulation of metals in the fixed-bed column is largely dependent on the quantity of sorbent inside the column. The sorption performance of olive stone was tested at various bed heights (bed depths), 300 g (21.5 cm), 600 g (42.5 cm), and 900 g (62.0 cm) at flow rate of 28 mL/min (these values have been selected to compare with the results obtained in laboratory-scale
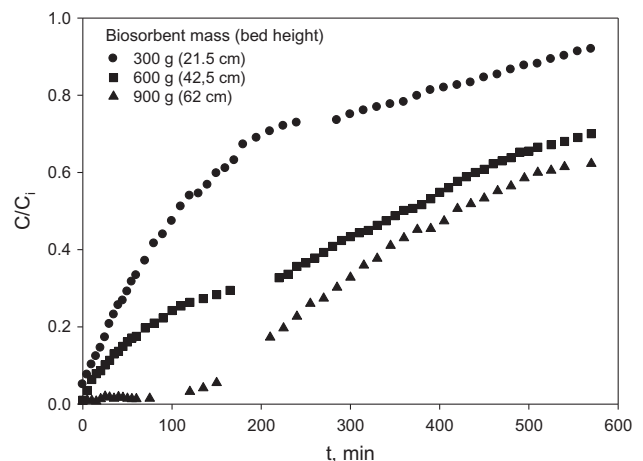

Fig. 2a. Cr(III) biosorption breakthrough curves by olive stone at three different bed heights (21.5, 42.5, and 62.0 cm).
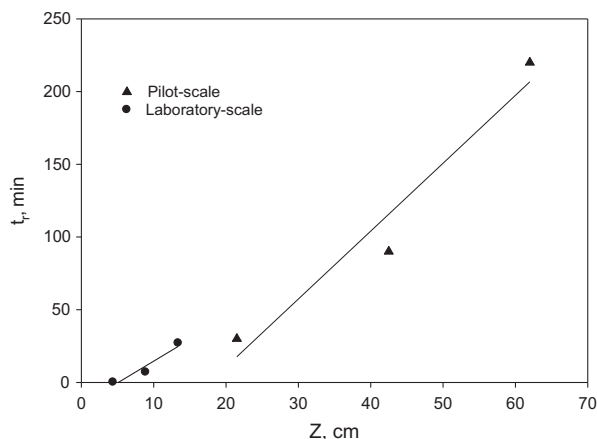
Fig. 2b. Fit of the BDST model for laboratory-scale column and pilot-scale column using equivalent operations conditions (Laboratory-scale: $C_i = 10$ mg/L; $Q = 4$ mL/min; Pilot-scale: $C_i = 10$ mg/L; $Q = 28$ mL/min).

columns) and inlet chromium concentration of 10 mg/L. Fig. 2a shows the breakthrough profile of chromium sorption at different bed heights.

As bed height increases, the amount of chromium removed (bed capacity) is also increased. The increase in biosorption with bed depth is due to the increase in biosorbent doses in larger beds which provide greater surface area (or biosorption sites, more binding sites available for biosorption). It is also manifested if the values of breakthrough time are observed, since breakthrough time varies from 30 to 220 min when the bed height increases from 21.5 to 62.0 cm, respectively. Similarly, the time necessary to reach the exhaustion of the column is increased with an increase of bed height, reaching exhaustion only for a mass of bed depth of 21.5 cm.

These results have been adjusted to bed depth service time (BDST) model. Equation of BDST model (Table 3) implies that the service time is a linear function of the bed depth (Z) and hence if service time is plotted against the bed depth at a flow rate of 28 mL/min and a initial chromium concentration of 10 mg/L, the N_0 (75.33 mg/L) and K_a (2.66×10^{-3} L/mg min) values can be obtained from the slope and the intercept, and an acceptable value for r^2 (0.95) indicated the validity of BDST model.

In a previous work with laboratory-scale columns, the sorption capacity of bed N_0 (67.68 mg/L) and K_a (14.43×10^{-3} L/mg min) values were obtained [22]. The sorption capacities of bed, N_0, are similar in both cases (laboratory and pilot scales), although slightly higher in pilot columns, which could indicate the reproducibility of the results to make the scale up. However, the value of the rate constant, K_a, which

characterizes the rate of solute transfer from the fluid phase to the solid phase, is lower in the pilot scale columns which could be associated with a slower rate of retention of chromium. If K_a is large, even a short adsorbent bed can avoid breakthrough, but as K_a decreases, a progressively longer adsorbent bed is required to avoid the breakthrough [23].

Fig. 2b shows the obtained fitting by BDST model for both columns, using equivalent operational conditions.

Furthermore, from the equation of BDST model (Table 3), when $C_i/C = 2$, that is, when the concentration in the effluent is equal to 50% of inlet concentration, which coincides with the point of inflection of the breakthrough curve since this model assumes that the curve is symmetrical [26], the logarithm is zero, and the expression is reduced to the following:

$$t_{50} = \frac{N_0 Z}{C_i v} \tag{7}$$

This equation corresponds to the equation of a straight line that passes through the origin. Fig. 3 shows the fit of this equation for both laboratory- and pilot scale columns.

Finally, Fig. 3 shows that in either case the straight line passes through the origin, existing a point of intersection with the "x" axis corresponds to a value of Z when $t_{50} = 0$. This depth value is called "critical bed depth" and it is the minimum bed length required to obtain the breakthrough time t_b at $t = 0$, namely, achieve the effluent concentration required by applicable law [24].
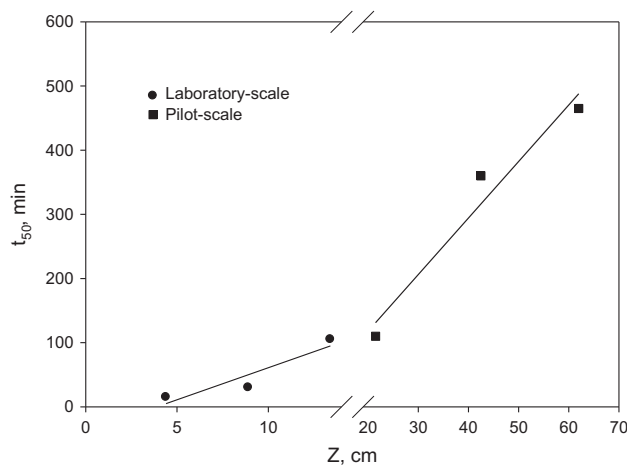

Fig. 3. Plots of t_{50} time vs. bed height of Cr(III) biosorption by olive stone for laboratory-scale and pilot-scale columns.
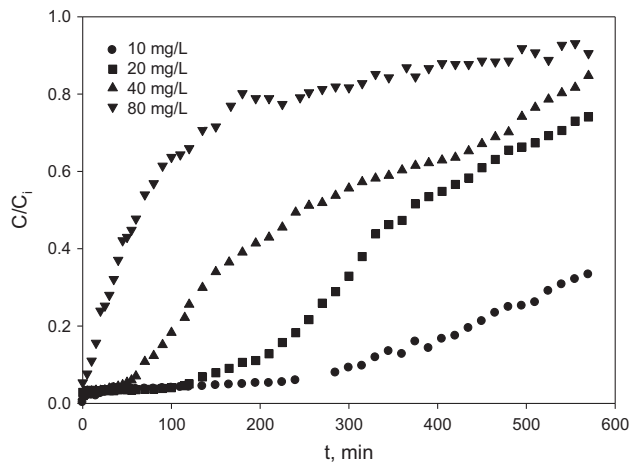
Fig. 4. Cr(III) biosorption breakthrough curves by olive stone at four different inlet chromium concentrations (10, 20, 40, and 80 mg/L).

Therefore, the critical bed depth can be calculated by setting $t = 0$ in Eq. (7). Thus, as expected critical bed length for laboratory-scale column was recorded as 3.8 cm compared to 6.6 cm for pilot-scale column. The results show that scale up multiplies by nearly 1.7 critical bed depth (the same relation that the ratio between Z/D of pilot scale column and laboratory column).

4.3. Effect of inlet Cr(III) concentration. Breakthrough curves: Modeling and determination of kinetic parameters

To determine the influence of the initial concentration of chromium, to describe the behavior of the column and to compare the results with those obtained previously at laboratory scale, mathematical models listed in Table 3 are applied and the corresponding kinetic parameters are determined.

In this respect, and considering the results obtained above, the following values have been chosen for the operational parameters: flow rate, 14 mL/min; pH 4; olive stone mass, 600 g (equivalent to a packing height of 42.5 cm); contact time, 600 min;

and initial concentrations of chromium, 10, 20, 40, and 80 mg/L. The results are shown in Fig. 4, and the parameters of breakthrough curves according Eqs. (1)–(6) are shown in Table 4.

As generally expected, a change in the inlet metal ion concentration of the feed affects the operating characteristics of the packed column. As the inlet concentration of chromium increases, the exhaustion of the column is reached earlier, requiring more than 570 min to concentrations of 10–20 mg/L. Higher initial chromium concentrations caused a faster breakthrough, as it was expected. A decrease in inlet Cr(III) concentrations gives delayed breakthrough curves and the treated volume was also higher, since the lower concentration gradient caused slower transport due to decreased diffusion coefficient [25]. At the highest Cr(III) concentration (80 mg/L), the olive stone bed is saturated quickly.

Also, biosorption capacity, q_e, increases as the inlet metal concentration increases from 0.146 to 0.305 mg/g for an inlet chromium concentration of 10–80 mg/L, respectively. In this point, it is necessary to specify that the biosorption capacity has been calculated at the same time for all concentrations and not at exhaustion time, due to it is not reached for concentration of 10–20 mg/L. However, the percentage of metal removed decreased significantly from 87.8 to 24.7% in the same range of concentrations.

It is also observed that the breakthrough time decreases significantly. For an initial concentration of 10 mg/L, it has a value of 415 min, while for an initial concentration of 80 mg/L, the breakthrough time is not reached (the exit concentration at time equal to zero is higher to breakthrough concentration). Therefore, for concentrations higher to 40 mg/L is necessary increasing the bed height or decreasing the flow rate to increase the breakthrough time.

Also, the exhaustion of the column is reached faster when the concentration increases. A time higher to 570 min it is needed for initial concentrations of 10–20 mg/L, while for a concentration of 80 mg/L, the exhausted time is reached at 330 min of the operational process.

Table 4
Parameters of breakthrough curves of the packed bed scale-pilot column for Cr(III) biosorption by olive stone at different inlet Cr(III) concentrations

C_i mg/L	t_b (min)	t_{ex} (min)	q_{total} (mg)	m_{total} (mg)	q_e (mg/g)	R (%)
10	415	>570	87.62	99.75	0.146	87.8
20	195	>570	99.87	149.23	0.167	66.9
40	45	565	177.77	339.95	0.296	52.3
80	–	330	182.70	740.54	0.305	24.7

Table 5
Adams–Bohart, Thomas, Yoon–Nelson, and Dose–Response model parameters at different inlet Cr(III) concentrations

| C_i (mg/L)	Adams–Bohart				Thomas				Yoon–Nelson				Dosis–Respuesta			
	k_{AB} (L/mg min)	N_0 (mg/L)	σ	r^2	k_{Th} (mL/min mg)	q_0 (mg/g)	σ	r^2	k_{YN} (min^{-1})	τ (min)	σ	r^2	a	q_0 (mg/g)	σ	r^2
10	0.000487	147.6	0.00269	0.956	0.565	0.161	0.00370	0.991	0.00564	687.8	0.00370	0.991	2.163	0.190	0.0223	0.947
20	0.000454	126.5	0.00108	0.965	0.451	0.174	0.0609	0.981	0.00844	398.5	0.0609	0.981	2.780	0.167	0.0261	0.992
40	0.000544	118.5	0.000563	0.974	0.166	0.302	0.2341	0.937	0.00706	302.9	0.2341	0.937	1.537	0.255	0.0326	0.991
80	0.000703	76.97	0.0000311	0.995	0.0907	0.300	0.4255	0.869	0.00841	138.8	0.4255	0.869	1.220	0.278	0.0870	0.895
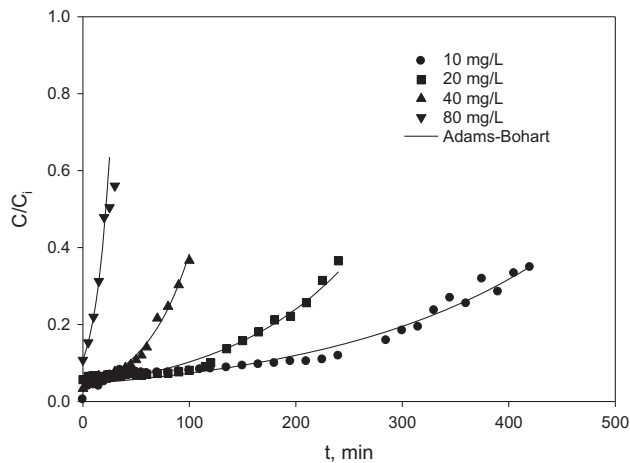
Fig. 5. The experimental and predicted breakthrough curves using the Adams–Bohart model for the biosorption of Cr(III) by olive stone at inlet chromium concentrations of 10, 20, 40, and 80 mg/L.
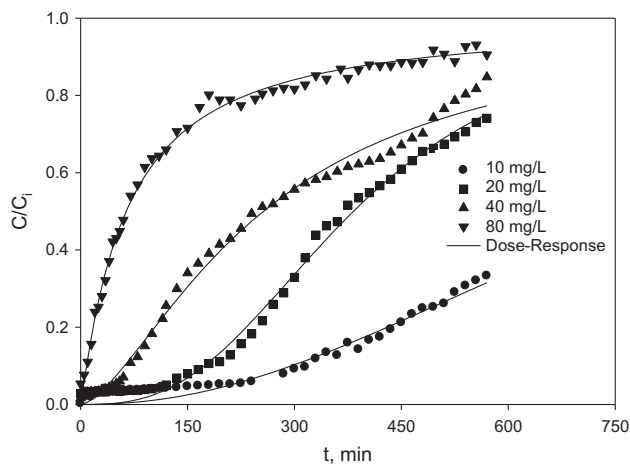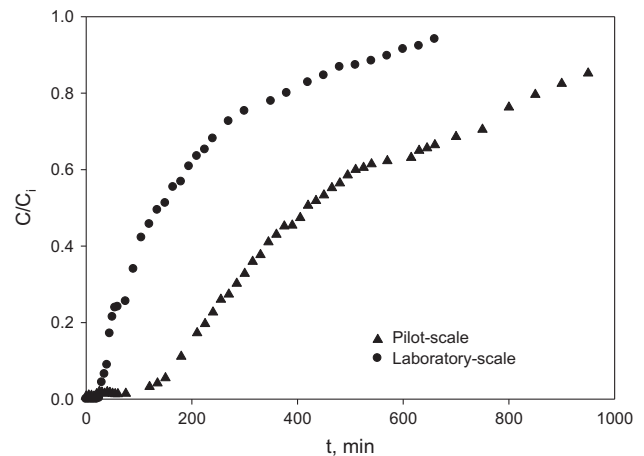

Fig. 7. Breakthrough curves of the pilot-scale and laboratory-scale columns in equivalent conditions: initial chromium concentration = 10 mg/L; feed flow = 4 mL/min (laboratory-scale) and 28 mL/min (pilot-scale); biosorbent dose= 15 g (laboratory-scale) and 900 g (pilot-scale).

Fig. 6. The experimental and predicted breakthrough curves using the Dose–Reponse model for the biosorption of Cr(III) by olive stone at inlet chromium concentrations of 10, 20, 40, and 80 mg/L.

These experimental results have been fitted by nonlinear regression to each of the previous models: Adams–Bohart, Thomas, Yoon–Nelson, and Dose–Response. Table 5 shows the values of the fitting parameters, the sum of squared deviations between experimental and calculated values ($\sigma = \sum((C/C_i)_{exp} - (C/C_i)_{cal})^2$) and the adjusted correlation coefficient (r^2).

Dose–Response model reproduced better experimental results for all initial chromium concentrations tested, just as in the tests performed on a laboratory scale. Moreover, the value of the chromium concentra-

tion in the solid phase, q_0, is very similar to the one obtained from the model of Thomas and the experimental value, being practically constant for all concentrations with a value near to 0.2 mg/g.

Likewise, the Adams–Bohart model can be used to reproduce the initial part of the breakthrough curve, just as in the laboratory-scale experiments. However, in pilot scale, the kinetic constant is slightly increased by raising the initial concentration of chromium, whereas at laboratory scale a slight decrease of the kinetic constant was observed for higher initial concentration of chromium. However, the order of magnitude of this parameter is the same in both types of tests.

The values of the parameter τ of Yoon–Nelson model that represents the time required to retain 50% of initial chromium ($C/C_i = 0.5$) (687.8, 399.4, 302.9, and 93.1 min, for 10, 20, 40, and 80 mg/L, respectively) are similar to those obtained experimentally (>570, 390, 270, and 75 min, for 10, 20, 40, and 80 mg/L, respectively).

In Figs. 5 and 6 the experimental data and the calculated values obtained with the Adams–Bohart model for the initial part of the curve and the Dose–Response model have been showed. A good fit of the experimental data by the Dose–Response model is observed, as previously indicated.

Comparing results obtained in the pilot-scale column with results obtained in laboratory-scale column [12] in Fig. 7, they represent the breakthrough curves to a performed experiment in both columns in equivalent conditions: initial chromium concentration = 10 mg/L;   feed   flow = 4 mL/min

(laboratory-scale) and 28 mL/min (pilot-scale); biosorbent dose = 15 g (laboratory-scale) and 900 g (pilot-scale).

Results show that retention process occurs faster in laboratory-scale columns. It is observed comparing the breakthrough and exhaustion times and the mass-transfer zone. The length of this zone is related to velocity of mass-transfer. For high velocities, the length is small, while for low velocities, the length is large. So, in laboratory-scale column, the breakthrough and exhaustion times are 42–480 min, respectively, and in pilot-scale column the breakthrough and exhaustion times are 220–950 min, respectively. Therefore, in pilot-scale column the mass-transfer zone is higher and it is related with a lower mass-transfer velocity.

On the other hand, it is observed that the percentage of chromium removal is higher in pilot-scale column, 59.3%, comparing to 32.6% obtained in laboratory-scale column. However, the behavior in the biosorption capacity at exhaustion time is the opposite, q_{ex} is lower in pilot-scale column (0.142 mg/g) than in laboratory-scale column (0.427 mg/g). Calculating the biosorption capacity at breakthrough time, this difference is lower (a value of 0.0597 mg/g for pilot-scale column and 0.0964 mg/g for laboratory-scale column). This difference may be due to that in the pilot-scale columns, the breakthrough time obtained was lower than it should have been obtained, according to the scale up [26,27].

From these results, the length of unused bed (LUB) can be obtained by Eq. (8) [24]:

$$\text{LUB} = L\left(1 - \frac{q_b}{q_{ex}}\right) \tag{8}$$

where q_b, y, q_{ex} are the biosorption capacities in the breakthrough and exhaustion time respectively (mg/g) and L is the total length of the bed column.

Using the Eq. (8) with data from both columns, it is obtained a value of LUB of 35.9 cm and 10.4 cm for pilot scale and laboratory scale, respectively. From LUB value it can be obtained the used fraction of the bed (FLB), as FLB = (L-LUB)/L and the breakthrough time, $t_b = t_{ex} \cdot$FLB. Obtained results are 0.42 for FLB and 399 min for t_b in pilot-scale column. These results confirm the comments indicated before.

In the same way, the obtained relation (L-LUB)/t_b, were 0.12–0.072 for pilot scale and laboratory-scale column respectively. These two values have a relation around 1.7.

This modeling of the pilot scale packed-bed column may allow the extrapolation to industrial units for the treatment of real industrial effluents.

5. Conclusions

The performance of the pilot scale fixed-bed column is very similar to the performance of the laboratory-scale fixed-bed column. Results show that it is possible to extrapolate to the industrial scale by using mathematical models obtained at pilot scale.

Effects of flow rate, bed depth, and initial chromium concentration on breakthrough curves were evaluated. The increase of the flow rate with constant solute concentration decreased the useful column operation time. Thus, as the fluid flow rate increased, the breakthrough and the exhaustion times decreased. Also, an increase on the biosorbent depth resulted in an increase in breakthrough time due to the presence of more sorbent material in the column and thus the higher sorption capacity of the system. The critical bed depth was also calculated, the results showed that scale up multiplied by nearly 1.7 critical bed depth. Finally, as the solute concentration increased, the saturation of the column occurred earlier, and thus an earlier breakthrough curve was obtained. The Adams–Bohart, the Thomas, the Yoon–Nelson, and the Dose–Response models were applied to experimental data obtained from dynamic studies performed on pilot-scale column to predict the breakthrough curves and to determine the column kinetic parameters. The initial region of breakthrough curve was defined by the Adams–Bohart model at all inlet Cr(III) concentrations studied while the full description of breakthrough could be accomplished by Dose–Response model. The LUB was also calculated and the results again show that scale up multiplied by nearly 1.7 this parameter.

References

[1] J.C. Moreno-Piraján, D. Rangel, B. Amaya, E.M. Vargasb, Design and construction of equipment to make adsorption at pilot plant scale of heavy metals, Z. Naturforsch. 63 (2008) 453–461.
[2] F. Hernáinz, M. Calero, G. Blázquez, M.A. Martín-Lara, Comparative study of the biosorption of cadmium(II), chromium (III), and lead(II) by olive stone, Environ. Prog. 27 (2008) 469–478.
[3] G. Blázquez, F. Hernáinz, M. Calero, M.A. Martín-Lara, G. Tenorio, The effect of pH on the biosorption of Cr(III) and Cr(VI) with olive stone, Chem. Eng. J. 148 (2009) 473–479.

[4] M.M. Montazer-Rahmati, P. Rabbani, A. Abdolali, A.R. Keshtkar, Kinetics and equilibrium studies on biosorption of cadmium, lead, and nickel ions from aqueous solutions by intact and chemically modified brown algae, J. Hazard. Mater. 185 (2011) 401–407.

[5] A. Ronda, M.A. Martín-Lara, M. Calero, G. Blázquez, Analysis of the kinetics of lead biosorption using native and chemically treatd olive tree pruning, Ecol. Eng. 58 (2013) 278–285.

[6] C. Wang, X. Ren, W. Li, Z. Hou, C. Ke, Q. Geng, Adsorption of zinc and copper heavy metal ions from smelting wastewater using modified lava particles, Pol. J. Environ. Stud. 22 (2013) 1863–1869.

[7] S. Kundu, A.K. Gupta, Analysis and modeling of fixed bed column operations on As(V) removal by adsorption onto iron oxide-coated cement (IOCC), J. Colloid Interface Sci. 290 (2005) 52–60.

[8] J.M. Smith, Chemical Engineering Kinetics, third ed., McGraw-Hill, International Editions, New Delhi, 1981.

[9] I. Mikhlyonov, A. Averbuch, E. Tumarkina, I. Furmer, Chemical Technology, Part I, third ed., MIR Publishers, Moscow, 1979.

[10] M.A. Martín-Lara, F. Hernáinz, M. Calero, G. Blázquez, G. Tenorio, Surface chemistry evaluation of some solid wastes from olive-oil industry used for lead removal from aqueous solutions, Biochem. Eng. J. 44 (2009) 151–159.

[11] M.A. Martín-Lara, G. Blázquez, A. Ronda, A. Pérez, M. Calero, Development and characterization of biosorbents To remove heavy metals from aqueous solutions by chemical treatment of olive stone, Ind. Eng. Chem. Res. 52 (2013) 10809–10819.

[12] M. Calero, F. Hernáinz, G. Blázquez, G. Tenorio, M.A. Martín-Lara, Study of Cr(III) biosorption in a fixed-bed column, J. Hazard. Mater. 171 (2009) 886–893.

[13] V.J. Inglezakis, S.G. Poulopoulous, Adsorption, Ion Exchange and Catalysis. Desig of Operations and Environmental Applications, Elsevier, Netherland, 2006.

[14] R.A. Hutchins, New method simplifies design of activated-carbon systems, Chem. Eng. 80 (1973) 133–138.

[15] G.S. Bohart, E.Q. Adams, Some aspects of the behaviour of the charcoal with respect chlorine, J. Am. Chem. Soc. 42 (1920) 523–544.

[16] H.C. Thomas, Heterogeneous ion exchange in a flowing system, J. Am. Chem. Soc. 66 (1944) 1664–1666.

[17] Z. Aksu, F. Gönen, Biosorption of phenol by immobilized activated sludge in a continuous packed bed: prediction of breakthrough curves, Process Biochem. 39 (2004) 599–613.

[18] Y.H. Yoon, J.H. Nelson, Application of gas adsorption kinetics I. A theorical model for respirator cartridge service life, Am. Ind. Hyg. Assoc. J. 45 (1984) 509–516.

[19] G.Y. Yan, T. Viraraghavan, M. Chem, A new model for heavy metal removal in a biosorption column, Adsorpt. Sci. Technol. 19 (2001) 25–43.

[20] R. Senthilkumar, K. Vijayaraghavan, M. Thilakavathi, P.V.R. Iyer, M. Velan, Seaweeds for the remediation of wastewaters contaminated with zinc (II) ions, J. Hazard. Mater. 136 (2006) 791–799.

[21] M. Karimi, A. Shojaei, A. Nematollahzadeh, M.J. Abdekhodaie, Column study of Cr(VI) adsorption onto modified silica–polyacrylamide microspheres composite, Chem. Eng. J. 210 (2012) 280–288.

[22] G. Tenorio, Caracterización de la biosorción de cromo con hueso de aceituna, PhD Thesis, University of Granada, Spain, 2006.

[23] R. Elagovan, L. Philip, K. Chandraraj, Biosorption of hexavalent and trivalent chromium by palm flower (Borassus aethiopum), Chem. Eng. J. 141 (2008) 99–111.

[24] D.O. Cooney, Adsorption Design for Wastewater Treatment, CRC Pres, Inc., Boca Raton (Florida), USA, 1999.

[25] T.V.N. Padmesh, K. Vijayaraghavan, G. Sekaran, M. Velan, Batch and column studies on biosorption of acid dyes on fresh water macro alga Azolla filiculoides, J. Hazard. Mater. 125 (2005) 121–129.

[26] K. Vijayaraghavan, Y.S. Yun, Polysulfone-immobilized Corynebacterium glutamicum: A biosorbent for reactive black five from aqueous solution in an up-flow packed column, Chem. Eng. J. 145 (2008) 44–49.

[27] S.H. Hasan, P. Srivastava, M. Talat, Biosorption of lead using immobilized Aeromonas hydrophila biomass in up flow column system: Factorial design for process optimization, J. Hazard. Mater. 177 (2010) 312–322.